Infrared reflectivity spectra of the reaction products K_xMoO_3 (x=0.1-0.5) prepared by a solid state reaction

1990 J. Phys.: Condens. Matter 2 5199

(http://iopscience.iop.org/0953-8984/2/23/010)

J. Phys.: Condens. Matter 2 (1990) 5199–5208. Printed in the UK

Infrared reflectivity spectra of the reaction products K_xMoO_3 ($x = 0.1$–0.5) prepared by a solid state reaction

T Hirata and K Yagisawa

National Research Institute for Metals, 2-3-12, Nakameguro, Meguro-ku, Tokyo 153, Japan

Received 18 December 1989, in final form 13 March 1990

Abstract. Infrared reflectivity spectra of the reaction products K_xMoO_3 prepared by a solid state reaction $[(x/2)K_2MoO_4 + (1-x)MoO_3 + (x/2)MoO_2 \rightarrow K_xMoO_3;\ x = 0.1$–$0.5]$ have been measured over the wavenumbers 400–4000 cm^{-1} at room temperature by means of Fourier transform infrared (FT-IR) microscopy.

Although x-ray diffractometry reveals that all reaction products are not of single phase, it turned out that three phonon peaks appear around 950 cm^{-1} in the spectra, and some spectral changes are observed depending on the potassium composition of the predominant phase in the reaction products which is determined by an EDAX SW 9100 spectrometer. The FT-IR microscope also confirms the 'phonon stiffening' in the transition from the 'blue bronze' ($K_{0.3}MoO_3$) to the 'red bronze' ($K_{0.33}MoO_3$), indicating a discontinuity in the plot of the wavenumbers for the three phonon peaks as a function of potassium composition. It is concluded that such a discontinuity is caused by a possibility that the Mo–O bond distances are shorter in $K_{0.33}MoO_3$ than in $K_{0.3}MoO_3$.

1. Introduction

Ternary transition metal oxides $M_xT_aO_b$ exhibit various structures and a variety of physical properties, depending on a variable amount x of a third element M, where M is usually an alkali metal or an alkaline-earth metal, which donates its electron(s) to the conduction band of the host metal. The potassium molybdenum bronze $K_{0.3}MoO_3$ or $K_{0.33}MoO_3$, the so-called 'blue bronze' or the 'red bronze', belongs to a class of ternary transition metal oxides. It is well known that $K_{0.3}MoO_3$ is a one-dimensional conductor along the crystallographic b axis and a metal–semiconductor transition of a Peierls type occurs at about 180 K (Perlstein and Sienko 1968, Travaglini *et al* 1981), whereas $K_{0.33}MoO_3$ is a highly anisotropic semiconductor at all temperatures (Travaglini and Wachter 1983, Travaglini *et al* 1982).

Travaglini *et al* (1981, 1982) have measured the optical reflectivity of these two bronzes on single crystals in the photon energy range 0.03–2 eV at temperatures 10–300 K using polarised light so as to study the metal–semiconductor transition; in our study we found three phonon peaks around 0.12 eV (968 cm^{-1}) and some anisotropy of the reflectivity shown by Travaglini *et al* (1981, 1982).

The structure of the blue bronze can be divided into fundamental groups of five octahedra which link by sharing edges to form a large sub-unit of ten octahedra; the sub-units join by sharing corners in two directions to form the infinite sheets of MoO_3 with

0953-8984/90/235199 + 12 $03.50

adjacent sheets being separated by K ions (Graham and Wadsley 1966). The red bronze consists of distorted Mo–O octahedra which are arranged to form a unit of six octahedra by sharing edges. These sub-units join by sharing corners to form the infinite sheets; large K ions are incorporated between these sheets (Stephnson and Wadsley 1965).

The above structure model predicts some changes in the vibration spectra of K_xMoO_3 depending on variable amounts of potassium, including K ions that bond with oxygen (Graham and Wadsley 1966, Stephnson and Wadsley 1965).

Thus, an attempt has been made to prepare the potassium molybdenum bronzes K_xMoO_3 with variable values of x and their infrared reflectivity spectra have been measured by means of FT-IR (Fourier transform infrared) microscopy, in order to confirm the above predictions; most of the research on the potassium molybdenum bronzes have been limited to K_xMoO_3 with $x = 0.3$ or $x = 0.33$.

2. Experimental details

The potassium molybdenum bronzes K_xMoO_3 were prepared by a solid state reaction according to:

$$(x/2)K_2MoO_4 + (1-x)MoO_3 + (x/2)MoO_2 \rightarrow K_xMoO_3. \quad (1)$$

Stoichiometric quantities of the reagent grade oxides, K_2MoO_4, MoO_3 and MoO_2, were weighed out to yield K_xMoO_3 with $x = 0.1$–0.5 (we set a limit of $x = 0.1$–0.5 as it is only possible to synthesise K_xMoO_3, with $x = 0.6$–1.0 under high pressure (Bither *et al* 1966)). Carefully ground and mixed reactants were pressed at 49 MPa into pellets with a diameter of 20 mm and a thickness 1–2 mm.

These pellets were subjected to CIP (cold isostatic pressing) at 196 MPa for the purpose of producing a higher degree of sintering. They were vacuum sealed in quartz tubes at a pressure of 10^{-5} Torr and sintered for 98 h at a temperature of 435 °C where all of the reactants remain solid.

Differential scanning calorimetry (DSC) on the mixtures was carried out with a DuPont 900 thermal analyser; an endothermic peak due to the melting of K_2MoO_4 was detected at 460 °C for each mixture, yielding K_xMoO_3 with variable values of x. The DSC curves showed some composition-dependent variations at temperatures of 475–600 °C. We could find no endothermic anomalies at 550 °C and ~610 °C as reported in the DTA analysis of the K_2MoO_4–MoO_3–MoO_2 mixture that would yield a composition $K_{0.35}MoO_3$ (Ramanujachary *et al* 1984).

Diffuse reflectance FT-IR spectra of K_2MoO_4 powders were measured during vacuum-annealing up to 450 °C, the results indicating no spectral changes except that atmospheric water vapour bands tended to disappear with an increase in temperature. In addition, no changes in the spectra of K_2MoO_4, MoO_2 and MoO_3 were observed before or after our sintering. Thus, we can consider that no decomposition or volatilisation of any reactant(s) occurred under our sample preparation conditions.

For phase identification and structural determination, x-ray diffractometry on the as-sintered pellets was carried out with Cu Kα radiation. Infrared reflectivity spectra were measured for the wavenumbers 400–4000 cm^{-1} at room temperature by means of a FT-IR microscope (JEOL 100). The FT-IR microscope is useful to measure infrared reflectivity spectra from a microscopic area of the sample that is of single phase and/or homogeneous composition. The spectrometer was run at a resolution of 4 cm^{-1} using two detectors: MCT ($Hg_{1-x}Cd_xTe$) or TGS (triglycine sulfate). The spectra were recorded

Table 1. The potassium composition in K_xMoO_3 ($x = 0.1$–0.5) determined by EDX spectroscopy.

x (nominal)	x_{exp}(I)†	x_{exp}(II)‡	x_{exp}(III)§
0.1	0.11	0.26	0.28
0.2	0.20	0.28	0.32
0.3	0.31	0.32	0.33
0.33	0.35	0.35	0.34
0.4	0.41	0.42‖	0.39
0.5	0.57	0.58‖	>0.45

† From an area of $1000 \times 800\ \mu m^2$.
‡ From an area of $100 \times 80\ \mu m^2$.
§ Average of at least three particles or more in point analysis.
‖ It is not well understood why $x_{exp}(II) > x$ in K_xMoO_3 with $x = 0.4$ and 0.5, so serious significance should not be attached to the values of $x_{exp}(II)$ in K_xMoO_3 with $x = 0.4$ and 0.5; however, the essence of our discussion is not influenced by this.

after 800 scans taking about 30 min; the infrared reflectivity spectrum of an evaporated Al thin film was also measured for reference, but raw spectra will be presented to demonstrate spectral features in the wavenumbers of interest.

An EDAX SW 9100 spectrometer was used to determine the potassium composition in K_xMoO_3, based on Mo Lα and K Kα lines using K_2MoO_4 for reference.

3. Results

3.1. Microstructure and colour

Figure 1 shows microstructure and colour of the reaction products K_xMoO_3 with the nominal composition: $x = 0.1$–0.5. In K_xMoO_3 with $x = 0.1$, 0.2 and 0.3, plate-like particles with a blue colour are observed, and at $x = 0.3$ they tend to become larger; these blue particles of various sizes are distributed over the whole gamut of the reaction products: K_xMoO_3 with $x = 0.1$–0.3.

In K_xMoO_3 with $x = 0.33$ and 0.4, platelets with a red colour are formed. We notice some large blue particles in K_xMoO_3 with $x = 0.33$, making it possible to measure infrared reflectivity spectra of a single particle with a blue or red colour. In K_xMoO_3 with $x = 0.5$, granular particles with a light blue colour are observed, suggesting the formation of a different phase from that formed in K_xMoO_3 with $x = 0.1$–0.4.

3.2. Determination of the potassium composition in K_xMoO_3

Table 1 shows the potassium composition in K_xMoO_3 determined from an area of $1000 \times 800\ \mu m^2$ or $100 \times 80\ \mu m^2$ and for such particles as shown in figure 1. The potassium composition determined from a wide area of the reaction products, x_{exp}(I), is close to the nominal composition in K_xMoO_3, whereas the potassium composition determined from a small area of the reaction products, x_{exp}(II), is equal to or larger than x_{exp}(I).

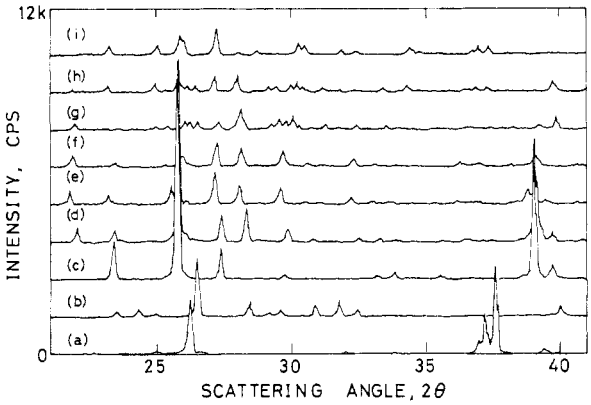

Figure 2. X-ray diffraction patterns (2θ: 21°–41°) for the reaction products K_xMoO_3 with $x = 0.1$–0.5 and the reactants, for comparison. (a) K_2MoO_4. (b) MoO_2. (c) MoO_3. (d) $x = 0.1$. (e) $x = 0.2$. (f) $x = 0.3$. (g) $x = 0.33$. (h) $x = 0.4$. (i) $x = 0.5$.

The values for x_{exp}(II) varied somewhat from place to place (chosen at random). Nevertheless, it is of particular interest to note that the potassium composition increases as $x_{exp}(II) \simeq 0.30$ with decreasing arbitrarily chosen areas in K_xMoO_3 when $x = 0.1$ and 0.2. This is due to the fact that the blue bronze $K_{0.3}MoO_3$ is formed preferentially in combination with another phase of a lower potassium composition, i.e. phase separation occurs during the solid state reaction to yield K_xMoO_3 with $x = 0.1$ and 0.2. More details of the potassium composition in K_xMoO_3 will be given elsewhere.

3.3. X-ray diffractometry

Figure 2 shows x-ray diffraction patterns for the reaction products K_xMoO_3 with $x = 0.1$–0.5 in the scattering angles: $2\theta = 21°$–$41°$; x-ray diffraction patterns for K_xMoO_4, MoO_2 and MoO_3 are also shown for comparison.

The following points should be noticed:

(i) The reactants, K_2MoO_4 and MoO_2, are absent in all reaction products, whereas MoO_3 remains to some extent in K_xMoO_3 when $x = 0.1$ and $x = 0.2$.

(ii) X-ray diffraction patterns for K_xMoO_3 with $x = 0.1$, 0.2 and 0.3 are basically similar, except for peak shifts and traces of a few peaks due to MoO_3.

(iii) X-ray diffraction patterns undergo a significant change between $x = 0.3$ and $x = 0.33$ and/or $x = 0.4$ (see around $2\theta = 27°$–$30°$); a comparison of figure 2(*h*) with figure 2(*i*) also reveals the disappearance and shift of a few peaks.

Structure and lattice parameters of the predominant phase in K_xMoO_3 with the nominal composition $x = 0.1$–0.5 are summarised in table 2.

The reaction product K_xMoO_3 with $x = 0.3$ is the blue bronze whose lattice parameters are comparable to those of Graham and Wadsley (1966) (cf Ghedira *et al* 1985). The predominant phase in K_xMoO_3 with $x = 0.33$ corresponds to the red bronze whose lattice parameters are in close agreement with Stephnson and Wadsley (1965). The structure of the predominant phase in K_xMoO_3 with $x = 0.5$ was determined to be tetragonal, and its lattice parameters are comparable to those of Bither *et al* (1966).

Table 2. Structures and lattice parameters of the predominant phase in K_xMoO_3 with the nominal composition: $x = 0.1$–0.5.

K_xMoO_3	Structure	Lattice parameters
$x = 0.1$	monoclinic	$a = 18.306$ Å
		$b = 7.556$ Å
		$c = 9.894$ Å
		$\beta = 117.93°$
$x = 0.2$	monoclinic	$a = 18.508$ Å
		$b = 7.625$ Å
		$c = 9.953$ Å
		$\beta = 117.88°$
$x = 0.3$	monoclinic	$a = 18.440$ Å
		$b = 7.599$ Å
		$c = 9.928$ Å
		$\beta = 117.88°$
$x = 0.33$	monoclinic	$a = 14.830$ Å
		$b = 7.721$ Å
		$c = 6.377$ Å
		$\beta = 92.58°$
$x = 0.4$	monoclinic	$a = 14.938$ Å
		$b = 7.796$ Å
		$c = 6.422$ Å
		$\beta = 92.38°$
$x = 0.5$	tetragonal	$a = 12.397$ Å
		$c = 3.841$ Å

X-ray diffractometry revealed that not all of the reaction products are of single phase; K_xMoO_3 with $x = 0.1$, 0.2 contains some amount of MoO_3, K_xMoO_3 with $x = 0.3$ is almost single phase, and K_xMoO_3 with $x = 0.33$, 0.4 and $x = 0.5$ contain traces of the blue bronzes and the red bronze, respectively.

Interplanar spacings or scattering angles for K_2MoO_4 and MoO_2, are in good agreement with those in the ASTM (American Society for Testing Materials) files: 29-1021 and 32-671, respectively. Scattering angles for MoO_3 also correspond to the ASTM file: 5-508 ($a = 3.954$ Å and $c = 13.847$ Å). The lattice parameters for MoO_3 in K_xMoO_3 with $x = 0.1$ and 0.2 are determined to be $a = 3.953$ Å, $c = 13.854$ Å and $a = 3.998$ Å, $c = 13.901$ Å respectively, indicating a lattice expansion of MoO_3 due to intercalation of K ions (Ramanujachary *et al* 1984).

Figure 3 shows a plot of the lattice parameters of the predominant phase in K_xMoO_3 as a function of $x_{exp}(II)$, which is considered to correspond to the potassium composition of the predominant phase in K_xMoO_3 with $x = 0.1$–0.4; the result for K_xMoO_3 with $x = 0.5$ is not plotted because the structure of the predominant phase in this reaction product is different. We can see that the lattice parameters a and/or c tend to increase slightly with $x_{exp}(II)$ outside $0.32 \leqslant x_{exp}(II) \leqslant 0.35$, whereas the lattice parameter b increases almost linearly with $x_{exp}(II)$. A sudden drop in a and c between $x_{exp}(II) = 0.32$ and $x_{exp}(II) = 0.35$ is attributed to a different set of crystallographic a and c axes in $K_{0.3}MoO_3$ and $K_{0.33}MoO_3$ (Graham and Wadsley 1966, Stephnson and Wadsley 1965).

3.4. Infrared reflectivity spectra

Figure 4(*a*) shows infrared reflectivity spectra of K_xMoO_3 with the nominal composition $x = 0.1$–0.5 between the wavenumbers 750–1100 cm^{-1}; these spectra are recorded from

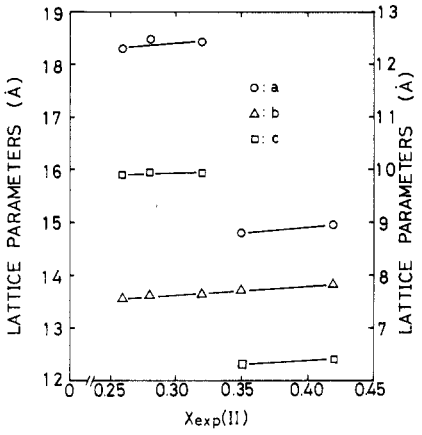

Figure 3. Plot of the lattice parameters (○ = *a*, △ = *b*, □ = *c*) as a function of x_{exp}(II), which is considered to correspond to the potassium composition of the predominant phase in K_xMoO_3 with $x = 0.1$–0.4; the lines are only drawn to guide the eye (left scale: for *a* and *c*, right scale: for *b*).

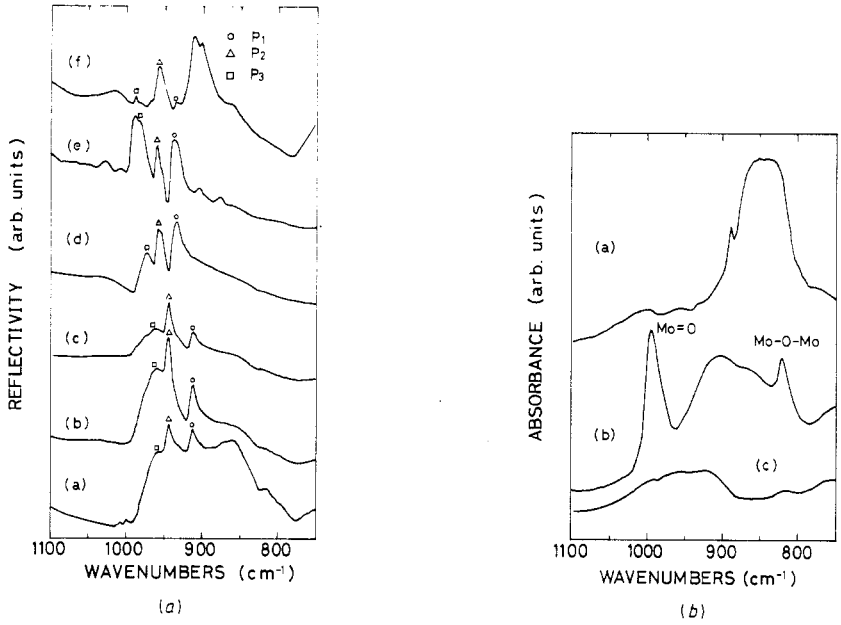

Figure 4. (*a*) Infrared reflectivity spectra of K_xMoO_3 with the nominal composition $x = 0.1$–0.5 between the wavenumbers 750–1100 cm^{-1}. (a) $x = 0.1$ (b) $x = 0.2$ (c) $x = 0.3$ (d) $x = 0.33$ (e) $x = 0.4$ (f) $x = 0.5$. (*b*) Infrared spectra of the reactants; (a) K_2MoO_4 (b) MoO_3 (c) MoO_2 between the wavenumbers 750–1100 cm^{-1}.

an area of 50 μm^2 of the reaction products, and no spectral features of interest are observed outside the wavenumbers mentioned above. Infrared spectra of K_2MoO_4, MoO_2 and MoO_3 are also shown in figure 4(*b*), for comparison. A comparison of figure 4(*a*) with figure 4(*b*) reveals that no bands due to K_2MoO_4 and MoO_2 are present in the spectra of K_xMoO_3 with $x = 0.1$–0.5, but that traces of the Mo–O–Mo bridging band at 820 cm^{-1} and the Mo=O terminal band at 999 cm^{-1} in MoO_3 (Seyedmonir *et al* 1982) are persistent in the spectra of K_xMoO_3 with $x = 0.1$–0.3 and $x = 0.1$, respectively. The

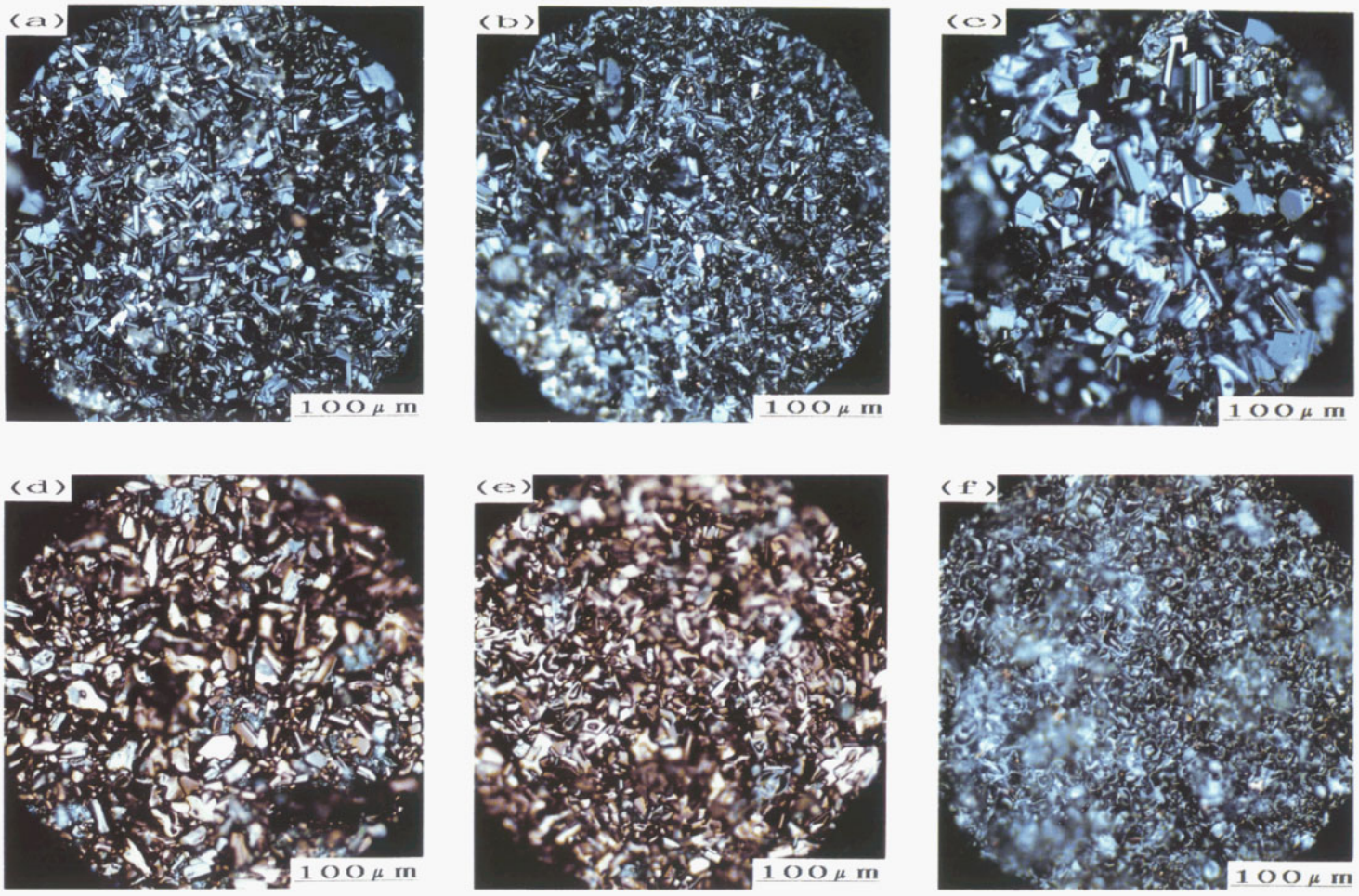

Figure 1. Microstructure and colour of the re ctio produc:s K_xMoO_3 with the nomi al composition $x = 0.1$–0.5. (*a*) $x = 0.1$ (*b*) $x = 0.2$ (*c*) $x = 0.3$ (*d*) $x = 0.33$ (*e*) $x = 0.4$ (*f*) $x = 0.5$.

Table 3. The wavenumbers of the peaks observed in the infrared reflectivity spectra of K_xMoO_3 with $x = 0.1$–0.5, with those of the Mo–O–Mo bridging band as well as the Mo=O terminal band in MoO_3: bd = broad, db = doublet and sh = shoulder.

K_xMoO_3	Wavenumbers (cm^{-1})	K_xMoO_3	Wavenumbers (cm^{-1})
$x = 0$ (MoO_3)	820 Mo–O–Mo	$x = 0.33$	933 ○
	904 bd		952 △] db
	994 Mo=O		957]
$x = 0.1$	820 Mo–O–Mo		973 □
	858 bd	$x = 0.4$	860 small
	911 ○		876
	943 △		903
	955 □		935 ○
	999] small		953 △ sh
	1008] db		958
$x = 0.2$	820 Mo–O–Mo		982 □]
	911 ○		988] db
	944 △		1007
	959 □		1028
$x = 0.3$	820 Mo–O–Mo	$x = 0.5$	858 bd
	911 ○		899] db
	944 △		909]
	961 □		933 ○
	986 sh		955 △
			986 □
			1018 bd

wavenumbers of the peaks observed in figure 4(*a*) are tabulated in table 3, with those of the Mo=O terminal band as well as the Mo–O–Mo bridging band in MoO_3. It is of interest to note that the peak positions and/or reflectivities of the three peaks labelled P_1, P_2 and P_3 in figure 4(*a*) depend on x in K_xMoO_3; we can also notice that the peaks P_1 and P_3 decay with the appearance of a doublet peak at ~900 cm^{-1}, in the spectrum of K_xMoO_3 with $x = 0.5$.

Figure 5 plots the wavenumbers of the three peaks, P_1, P_2 and P_3 as a function of $x_{exp}(II)$. It is evident that there is a discontinuity in the plot between $x_{exp}(II) \simeq 0.32$ and $x_{exp}(II) \simeq 0.35$. The peak, P_3, shifts upwards substantially with $x_{exp}(II)$, and the peak, P_2, also tends to shift upwards slightly with $x_{exp}(II)$.

Figure 6 shows infrared reflectivity spectra of a single particle (25 μm^2) with either a blue or red colour in K_xMoO_3 with $x = 0.33$, which we believe corresponds to the so-called blue bronze ($K_{0.3}MoO_3$) or the red bronze ($K_{0.33}MoO_3$).

The wavenumbers of the peaks in figure 6(*a*) and (*b*) are in good agreement with those in the spectra of K_xMoO_3 with $x = 0.3$ and $x = 0.4$ in figure 4(*a*), respectively. Thus, we can easily match these peaks against the three peaks P_1, P_2 and P_3 in figure 4(*a*), indicating the phonon stiffening in the transition from the blue bronze to the red bronze.

4. Discussion

The blue bronze as well as the red bronze crystallises in the monoclinic space group C2/m (Graham and Wadsley 1966, Stephnson and Wadsley 1965). A group theoretical

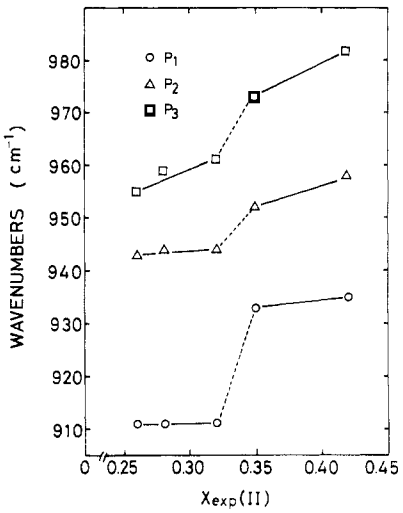

Figure 5. Plot of the wavenumbers of the three peaks P_1, P_2 and P_3 as shown in figure 4(*a*), as a function of x_{exp}(II).

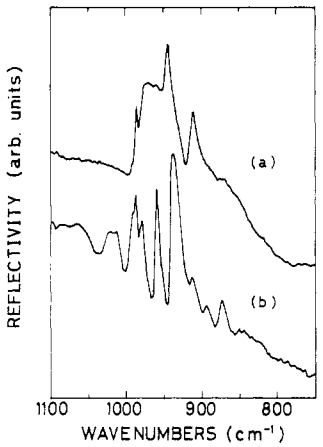

Figure 6. Infrared reflectivity spectra of a single particle (25 μm^2) with a blue or red colour (a; blue, b; red) in K_xMoO_3 with $x = 0.33$.

analysis gives the irreducible representation of vibrational modes for an octahedral MoO_6 as follows:

$$\chi_v = 4A_g(R) + 2B_g(R) + 3A_u(IR) + 6B_u(IR)$$

where the symmetry species A_g and B_g are Raman active whereas the two others A_u and B_u are infrared active. It seems difficult to make a realistic phonon analysis for the two bronzes, because of the large number of atoms in the unit cell (6 K + 20 Mo + 60 O = 86 for $K_{0.3}MoO_3$; 4 K + 12 Mo + 36 O = 52 for $K_{0.33}MoO_3$), in addition to that the sub-units of 10 or 6 MoO_6 octahedra are formed with some distortion.

In the present work, we mostly pay attention to the phonon stiffening in the transition from the blue bronze to the red bronze, and to the role of K incorporation. Assuming a bond-scaling relationship (Maroni *et al* 1989), the bond strength or the spring constant is reduced to Mo–O interatomic distances. In $K_{0.3}MoO_3$ with three crystallographically independent Mo sites: 4(i) for Mo(1), 8(j) for Mo(2) and Mo(3), the Mo–O interatomic distances are reported to be: Mo(1)–O; 1.68–2.30 Å, Mo(2)–O; 1.73–2.06 Å, and Mo(3)–O; 1.72–2.31 Å (Graham and Wadsley 1966, Ghedira *et al* 1985). On the other hand, the Mo–O interatomic distances in $K_{0.33}MoO_3$ with two Mo sites: 4(i) for Mo(1) and 8(j) for Mo(2) are as follows: Mo(1)–O; 1.67–2.56 Å and Mo(2)–O; 1.87–2.35 Å (Stephnson and Wadsley 1965).

Thus, a comparison of the Mo–O interatomic distances in $K_{0.3}MoO_3$ with those in $K_{0.33}MoO_3$, fails to account for the phonon stiffening in the transition from the blue bronze to the red bronze. However, it is probable that the Mo–O interatomic distances would be shorter in the red bronze than the blue bronze, for two reasons.

Firstly, an inspection of figures 2 in Travaglini *et al* (1981, 1982) confirms the phonon stiffening in the transition from $K_{0.3}MoO_3$ to $K_{0.33}MoO_3$. Secondly, the bond strength/length analysis (Zachariasen 1978) yields a lower valence $<Mo^{5+}$ on the two Mo sites (4.79 and 4.82) which causes a breakdown of charge neutrality for $K_{0.33}MoO_3$ with K^{1+}

and O^{2-}, whereas the Mo–O interatomic distances in $K_{0.3}MoO_3$ give rise to a charge distribution between Mo^{5+} and Mo^{6+}, preserving charge neutrality.

Applying an empirical rule, $\nu d^3 = \text{constant}$ (Lucovsky 1979), where ν is a vibrational frequency and d is the interatomic spacing, the discontinuity as shown in figure 5 yields the Mo–O interatomic distances shorter by about 1% in the red bronze than the blue bronze; the above empirical equation is strictly inapplicable to know variations in the Mo–O interatomic distances in view of different potassium compositions between the discontinuity, however, it can estimate some changes in the Mo–O interatomic distances in disregard of the effect of the slightly different potassium composition in the blue bronze and the red bronze with the same structure.

We conjecture that this small decrease in the Mo–O interatomic distances takes place along the *a*- and /or *c*-axis, because the lattice parameter *b* increases almost linearly through the transition region from the blue bronze to the red bronze (figure 3); in fact, Travaglini and Wachter (1983) showed that the Mo–O interatomic distances along the *b* axis are about 6% larger in $K_{0.33}MoO_3$ than $K_{0.3}MoO_3$. Figure 3 also indicates that the lattice parameter *a* as well as *c* tends to increase slightly with $x_{exp}(II)$ outside $0.32 < x_{exp}(II) < 0.35$. This reflects some variations in the potassium composition of the predominant phase in K_xMoO_3 with $x = 0.1$–0.4. Since the peak P_3 shifts upwards substantially with $x_{exp}(II)$ and as we know that our infrared spectra are due to the predominant phase in K_xMoO_3 whose structure and lattice parameters are determined by x-ray diffractometry, it follows that the phonon peaks in question are influenced by the incorporation of K ions that bond with oxygen. Solid state reactions have a potential for producing molybdenum bronzes with a potassium composition different from that in the blue bronze and/or the red bronze.

The B_u vibration involves the atomic motion within the plane containing 4 oxygens with Mo as the centre in an MoO_6 octahedron, whereas the A_u vibration involves the atomic motion out of the plane (the character of B_u or A_u is $+1$ or -1 with respect to σ_h).

In view of the discontinuity in the plot of the peak positions as a function of potassium composition that is caused by the shorter Mo–O interatomic distances in $K_{0.33}MoO_3$ than in $K_{0.3}MoO_3$ along the *a*- and/or *c*-axis, i.e., within the plane mentioned above we can assign the three peaks in figure 4(*a*) to the B_u vibration. In fact, the crystallites grow in the *b* axis direction and the IR light is perpendicular to the *b* axis in our infrared reflectivity measurements so that the three phonon peaks are observable (Travaglini *et al* 1981, 1982, Travaglini and Wachter 1983).

Finally, it is of particular interest to measure the infrared reflectivity spectra of K_xMoO_3 with $x = 0.1$–0.5 at various temperatures from 300 K to 10 K, in an expanded spectral region including far- and near-infrared; it is also interesting to measure physical properties of the molybdenum bronzes with variable amounts of potassium, in spite of the two-phase nature of the reaction products.

Acknowledgments

We thank Messrs M Otaguchi, H Doi, M Kadoi and Y Fukuda for CIP, x-ray diffractometry, vacuum-sealing of the pellets into quartz tubes and the determination of the potassium composition in K_xMoO_3, respectively. We are also grateful to Dr T Matsumoto for allowing the use of a computer program to calculate lattice parameters

and to Drs M Okochi and A Yoshikawa for their continuous encouragement during this work.

References

Bither T A, Gillson J L and Young H S 1966 *Inorg. Chem.* **5** 1559
Ghedira M, Chenavas J, Marezio M and Marcus J 1985 *J. Solid State Chem.* **57** 300
Graham J and Wadsley A D 1966 *Acta Crystallogr.* **20** 93
Lucovsky G 1979 *Solid State Commun.* **29** 571
Maroni V A, Brun T O, Grimsditch M and Loong C K 1989 *Phys. Rev.* B **39** 4127
Perlstein J H and Sienko M J 1968 *J. Chem. Phys.* **48** 174
Ramanujachary K V, Greenblatt M and Mccarroll W H 1984 *J. Cryst. Growth* **70** 476
Seyedmonir S R, Abdo S and Howe R F 1982 *J. Phys. Chem. Lett.* **86** 1233
Stephnson N C and Wadsley A D 1965 *Acta Crystallogr.* **18** 241
Travaglini G and Wachter P 1983 *Solid State Commun.* **47** 217
Travaglini G, Wachter P, Marcus J and Schlenker C 1981 *Solid State Commun.* **37** 599
—— 1982 *Solid State Commun.* **42** 407
Zachariasen W H 1978 *J. Less-Common Met.* **62** 1